



Synthesis and photovoltaic properties of thieno[3,2-b]thiophenyl substituted benzo[1,2-b:4,5-b']dithiophene copolymers

Journal:	<i>Polymer Chemistry</i>
Manuscript ID:	PY-ART-06-2014-000827.R1
Article Type:	Paper
Date Submitted by the Author:	22-Jul-2014
Complete List of Authors:	Xiao, Ze-Yun; University of Melbourne, Chemistry Subbiah, Jegadesan; University of Melbourne, Chemistry Sun, Kuan; University of Melbourne, Chemistry Jones, David; University of Melbourne, Chemistry/Bio21 Holmes, Andrew; University of Melbourne, Chemistry Wong, Wallace; University of Melbourne, Chemistry

Cite this: DOI: 10.1039/c0xx00000x

www.rsc.org/xxxxxx

ARTICLE TYPE

Synthesis and photovoltaic properties of thieno[3,2-*b*]thiophenyl substituted benzo[1,2-*b*:4,5-*b'*]dithiophene copolymers

Zeyun Xiao,^a Jegadesan Subbiah,^a Kuan Sun,^a David J. Jones,^a Andrew B. Holmes^a and Wallace W. H. Wong^{*a}

Received (in XXX, XXX) Xth XXXXXXXXX 20XX, Accepted Xth XXXXXXXXX 20XX
DOI: 10.1039/b000000x

A new benzo[1,2-*b*:4,5-*b'*]dithiophene (BDT) building block with 4,8-disubstitution using 2-(2-ethylhexyl)-3-hexylthieno[3,2-*b*]thiophene as the substituent has been designed and synthesized. The new building block has been copolymerized with benzothiadiazole (BT) and 5,6-difluorobenzothiadiazole (fBT) by Suzuki and Stille coupling polymerization to synthesize donor-acceptor conjugated polymers. The optical and electrochemical properties of the synthesized copolymers were studied. Bulk heterojunction solar cells were fabricated using the donor-acceptor copolymers in conjunction with PC₇₁BM and exhibited up to 4.20% power conversion efficiency.

Introduction

Bulk heterojunction (BHJ) polymer solar cells consisting of a blend of conjugated polymer donor and a fullerene acceptor as the photoactive layer have attracted considerable attention during the last decade.¹⁻⁷ Materials innovation, especially the development of the conjugated polymer donor, is one of the major forces that has driven the improvements in device performance reaching power conversion efficiency (PCE) of over 9%.⁵⁻⁷

Among various conjugated polymers developed for BHJ solar cells, the two-dimensional conjugated (“2D conjugated”) polymers, in which conjugated side chains are orthogonally attached to the polymer backbone, are particularly interesting due to their superior optical and electrical properties.⁸⁻¹⁰ One of the most successful examples of this concept has been demonstrated on polymers containing benzo[1,2-*b*:4,5-*b'*]dithiophene (BDT) building block on their backbone.¹¹ The “2D conjugated” polymers exhibited red-shifted absorption spectra, significantly higher hole mobility, and greatly improved photovoltaic properties, in comparison with the two alkoxy substituted polymer analogues.^{1,11}

Meanwhile, extending the fused-rings systems along the polymer backbone can also lead to enhancement in the optical absorption profile, charge carrier mobility, and BHJ solar cell performance.⁵⁻⁷ In a polymer system containing the dithieno[2,3-*d*:2',3'-*d'*]benzo[1,2-*b*:4,5-*b'*]dithiophene (Fig. 1) building block, it was hypothesised that the device performance improvement was a result of lower positive charge density and exciton binding energy.¹² In another system, the π -conjugation of indacenodithiophene unit was extended by incorporating thieno[3,2-*b*]thiophene units to form the indacenodithieno[3,2-*b*]thiophene donor moiety (Fig. 1) which had longer effective conjugation and better planarity resulting in improved charge

mobility.¹³ Dithienogermole has also been extended by incorporating thieno[3,2-*b*]thiophene with the aim of enforcing coplanarity, reducing rotational disorder, lowering reorganization energy and increasing charge carrier mobility (Fig. 1).¹⁴

Literature work: extending fused-ring system along polymer backbone

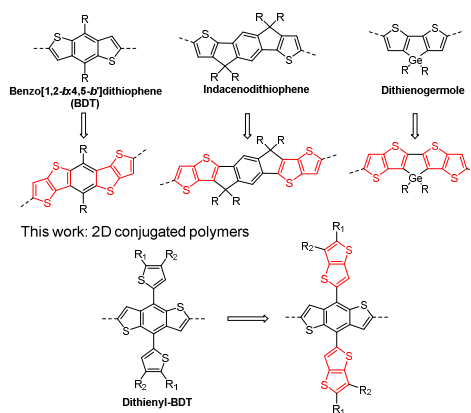
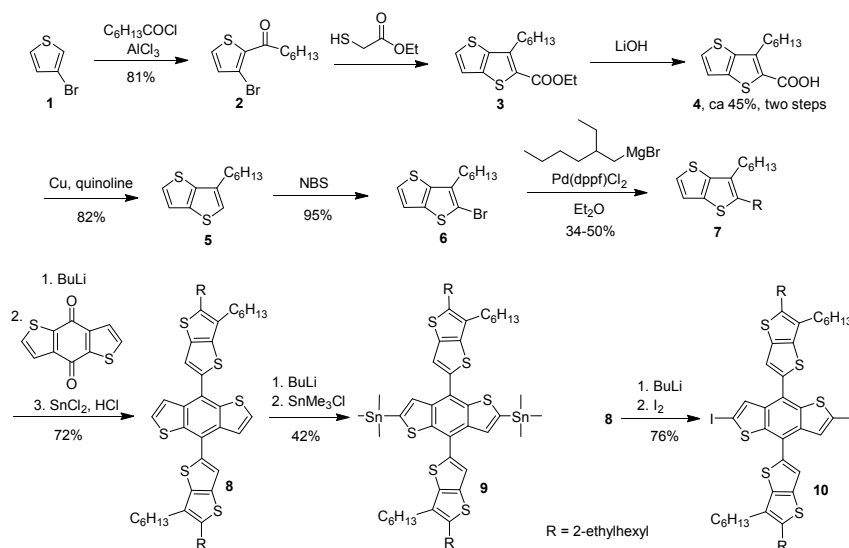


Fig. 1 Schematic illustrations of substituting thiophene with thieno[3,2-*b*]thiophene along polymer backbone and in a 2D conjugated manner.

In BHJ polymer solar cells, BDT based copolymers are among the most frequently used donor materials.¹⁵⁻¹⁸ A number of dithienyl-BDT containing polymers have been used in high performance solar cell devices (Fig. 1).¹⁹ In this study, the orthogonal thiophene units on the BDT core was replaced by thieno[3,2-*b*]thiophene units (Fig. 1). It was envisaged that the introduction of two alkyl chains on the thieno[3,2-*b*]thiophene units would provide the solution processability required for material characterisation and device fabrication.²⁰ Extending of the fused ring system in the 2D direction is expected to broaden the light absorption of the material with enhanced high energy absorption bands. In addition, the 2D conjugation would allow the delocalization of holes over the side chain, thus lowering



Scheme 1 Synthetic routes to the thieno[3,2-b]thiophene substituted BDT monomers.

the local charge density and the Coulombic interactions between the hole and the electron in the donor-acceptor interface.²¹⁻²³

5 Compared with extending the fused-ring systems along the polymer backbone, the extending of a fused ring in the side chains could also maintain the solubility and processability of the conjugated polymers. To achieve low highest occupied molecular orbital (HOMO) energy level and thus the high open circuit
10 voltage (V_{oc}), benzothiadiazole (BT) and 5,6-difluoro-2,1,3-benzothiadiazole (fBT) were used as the acceptor units for the synthesis of the donor-acceptor conjugated polymers.^{13, 19, 24-27}

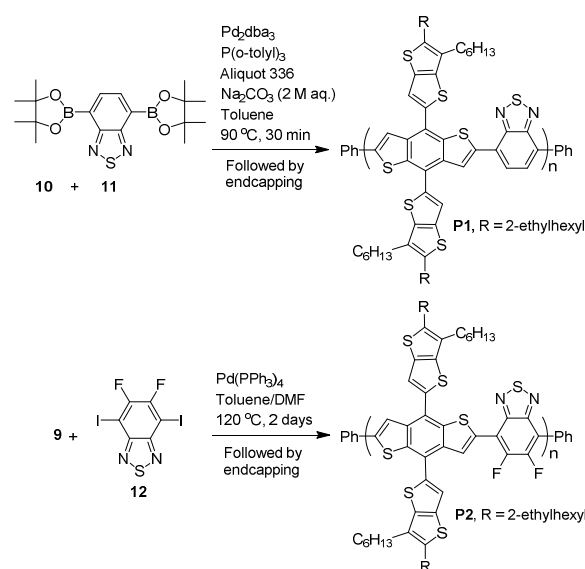
Synthesis and characterization

Monomer and polymer synthesis

15 The synthetic route for preparing the 4,8-bis(2-(2-ethylhexyl)-3-hexylthieno[3,2-b]thiophene) BDT monomers is shown in Scheme 1. 2-(2-(2-Ethylhexyl)-3-hexylthieno[3,2-b]thiophene) BDT monomers was obtained by Kumada coupling of 2-bromo-3-hexylthieno[3,2-b]thiophene **6** and 2-ethylhexyl bromide with the catalyst of
20 Pd(dppf)Cl₂. After deprotonation with butyl lithium, compound **7** was treated with 4,8-dihydrobenzo[1,2-b:4,5-b']dithiophene-4,8-dione and then reduced with tin(II) chloride to give BDT **8** in 72% yield. Compound **8** was converted into the diiodo monomer **10** or bistrimethylstannyl monomer **9** with *n*-butyl lithium and
25 then iodine or trimethyltin chloride.

The copolymerization of the diiodo monomer **10** and the BT monomer **11** by Suzuki coupling polymerization was very efficient (Scheme 2).²⁸ Polymerization time of 0.5 hour was enough for high MW polymer and further increase of the
30 polymerization time lead to large quantity of insoluble polymer. The resulting polymer was purified by precipitation from methanol and subsequent Soxhlet extraction with methanol, acetone, hexane, dichloromethane, and chloroform. The fBT monomer **12** is not stable in the hot basic condition employed in
35 the Suzuki coupling polymerization, so the fBT monomer **12** was copolymerized with the bistrimethylstannyl monomer **9** by Stille

coupling polymerization (Scheme 2).²⁹ In comparison with the Suzuki coupling polymerization, the Stille coupling polymerization was much slower and took 2 days. The resulting
40 polymer **P2** was purified in a similar way to that of the polymer **P1**. The yields of **P1** and **P2** were 43% and 39%, respectively. Polymers **P1** and **P2** were soluble in chlorinated solvent such as chlorobenzene and *o*-dichlorobenzene, but not soluble in acetone, toluene, hexane or acetonitrile. The molecular weight and
45 polydispersity (PDI) of the polymers were determined using high temperature gel-permeation chromatography (GPC) in trichlorobenzene at 120 °C (Figures S1 and S2). The number-average molecular weight (M_n) of **P1** and **P2** were 28,900 and 10,500 g/mol, respectively. Thermal properties of the polymers
50 were investigated using differential scanning calorimetry (DSC). No significant thermal transitions were observed in DSC analysis in the range of 40 to 300 °C for both polymers (Fig. S3).



Scheme 2 Synthesis of the polymers **P1** and **P2**.

Table 1 The optical properties and electronic energy levels of the polymers **P1** and **P2**.

polymer	Molecular weight (g/mol) ^a	UV-vis λ_{\max} (nm) ^b	Absorption coefficient at λ_{\max} ($L\ g^{-1}\ cm^{-1}$) ^c	UV-vis λ_{onset} (nm) ^d	Optical energy gap (eV) ^e	PL λ_{\max} (nm) ^f	E_{HOMO} (eV) ^g	E_{LUMO} (eV) ^g	HOMO-LUMO gap by CV (eV)
P1	28,900 (1.9)	648 (652)	16.7	731 (740)	1.68	720 (725)	-5.46	-3.61	1.85
P2	10,500 (3.3)	644 (657)	16.9	740 (747)	1.66	707 (716)	-5.50	-3.68	1.82

^a Molecular weight data obtained by GPC calibrated against polystyrene standards with polydispersity index in brackets. ^b UV-vis absorption maxima in chloroform solution and as thin films in bracket. ^c Calculated at the absorption maximum in chloroform solution (0.04 g/L). ^d UV-vis onset absorption in chloroform solution and as thin films in bracket. ^e Calculated from thin film absorption onset. ^f Fluorescence emission maxima in chloroform solution and as thin films in bracket. ^g Measured using cyclic voltammetry.

Optical properties and energy levels

The UV-vis absorption spectra of the polymers in chloroform are shown in Fig. 2a. Both polymers exhibited broad absorption from 300 nm to 700 nm. The absorption maximum (λ_{\max}) of **P1** was located at 648 nm and the onset absorption (λ_{onset}) was at 731 nm (Table 1). Polymer **P2** showed slightly red shifted λ_{onset} due to the more electron withdrawing properties of the fBT unit (the λ_{\max} and λ_{onset} of **P2** were at 644 and 740 nm, respectively). The longest wavelength absorption band could be assigned to the intramolecular charge transfer (ICT) between the acceptor units and the donor BDT units in the main chain. A significant difference of the absorptions of the two polymers was that **P2** displayed a stronger absorption peak at 501 nm. **P2** had a lower molecular weight and a stronger electron push-pull property between the BDT unit and the difluoro substituted fBT unit, so the peak at 501 nm was more obvious than that of the **P1**.^{30, 31}

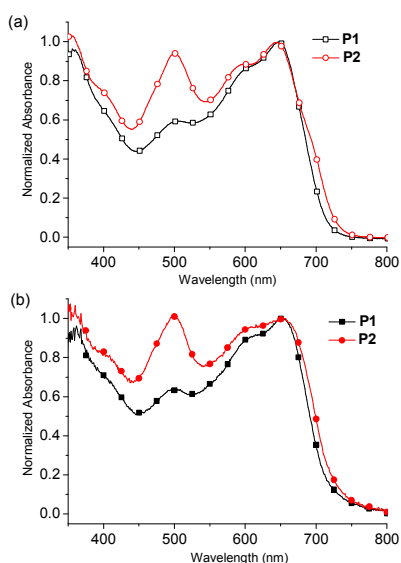


Fig. 2 Normalized UV-vis absorption spectrum of polymers **P1** and **P2** (a) in chloroform solution and (b) in the solid films.

P1 and **P2** showed solid film absorptions similar to their solution absorptions (Fig. 2b). Compared with the solution absorption, the λ_{\max} of the **P1** film only red-shifted 4 nm. The relatively low red-shift indicated that the polymers had a rigid-rod confirmation in both solution and solid state.^{32, 33} The λ_{\max} of the **P2** film red-shifted 13 nm suggesting aggregation and higher ordering in the solid state. By extrapolating the absorption edges of the film absorption, the λ_{onset} of the **P1** and **P2** films was determined to be 740 nm and 747 nm respectively. This

corresponds to an optical energy gaps of 1.68 eV for **P1** and 1.66 eV for **P2** (Table 1). **P1** and **P2** showed solution fluorescence emission maximum at 720 and 707 nm respectively when photo-excited at 650 nm. Very weak solid film fluorescence emission was recorded at 725 and 716 nm for **P1** and **P2** film, respectively (Table 1 and Fig. S4).

Electrochemical properties of the polymers were investigated via cyclic voltammetry (CV) using a three-electrode cell with a glass carbon working electrode, a platinum wire counter electrode, and an Ag/Ag⁺ pseudo reference electrode (Fig. 3). Ferrocene was used as the internal reference. The measurements were performed in an acetonitrile solution containing 0.1 M Bu₄NPF₆ at a scan rate of 50 mV s⁻¹. Film samples prepared by drop-casting *o*-dichlorobenzene solutions of the polymers onto the glass carbon electrode. Polymer **P1** showed irreversible oxidation peak around at 0.98 V, while **P2** displayed a slight higher irreversible oxidation peak of 1.02 V (Fig. 3). The onset potentials of the oxidation were used to calculate the HOMO energy levels for the polymers. Using the ferrocene/ferrocenium (Fc/Fc⁺) redox couple as reference (4.8 eV below vacuum), the HOMO energy levels of the **P1** and **P2** were determined at -5.46 eV and -5.50 eV, respectively.³⁴ The onset reduction potentials were used to calculate the LUMO energy levels which were at -3.61 eV and -3.68 eV for **P1** and **P2**, respectively (Table 1). The HOMO-LUMO energy gap measured from these electrochemical experiments were slightly larger than the optical energy gap (Table 1).^{17, 35} From the CV measurement results, both polymers showed low lying HOMO energy levels which is good for achieving high V_{oc} solar cells.³⁶ The introduction of the fluorine atom only caused a small perturbation in the HOMO energy level of the resulting polymer.

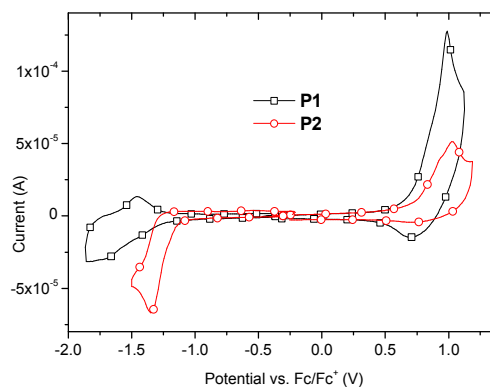


Fig. 3 Cyclic voltammetry curves showing oxidation and reduction processes of polymer films.

Device fabrication and characterization

The photovoltaic device performance of polymers **P1** and **P2** were investigated. A schematic diagram of the solar cells with inverted device architecture [ITO/ZnO/active layer/MoO₃/Ag] is shown in Fig. 4a. *o*-Dichlorobenzene (*o*DCB) was chosen as the processing solvent due to its good solvent properties and low evaporation rates. Optimized blend ratio of polymer/PC₇₁BM 1:2 was used for spin coating of the active layer. The blend film absorption is shown in Fig. S5. The devices were studied under the illumination of AM 1.5 G, 100 mW cm⁻². The current density to voltage (*J-V*) curves of the polymer/PC₇₁BM devices are displayed in Fig. 4b and the photovoltaic performance is listed in Table 2. The **P1**:PC₇₁BM (1:2) devices showed an average PCE of 2.6% with a *V*_{oc} of 0.90 V, a fill factor (FF) of 42%, and a short circuit current density (*J*_{sc}) of 6.8 mA cm⁻². The use of solvent additive, 1,8-diiodooctane (DIO), was found to be very effective in improving the device performance.³⁷⁻³⁹ With 2.5% (volume ratio) of DIO in the processing solvent *o*DCB, the BHJ solar cell performance increased by 40% with a greatly improved *J*_{sc} of 10.2 mA cm⁻² leading to PCE of 3.90% (Table S1). The increasing of the *J*_{sc} and the FF could be due to the improved morphology as evidenced by morphology studies (*vide infra*). Thermal annealing of the DIO processed solar cells at 120 °C for 3 minutes further increased the PCE to 4.20% (Table 2).

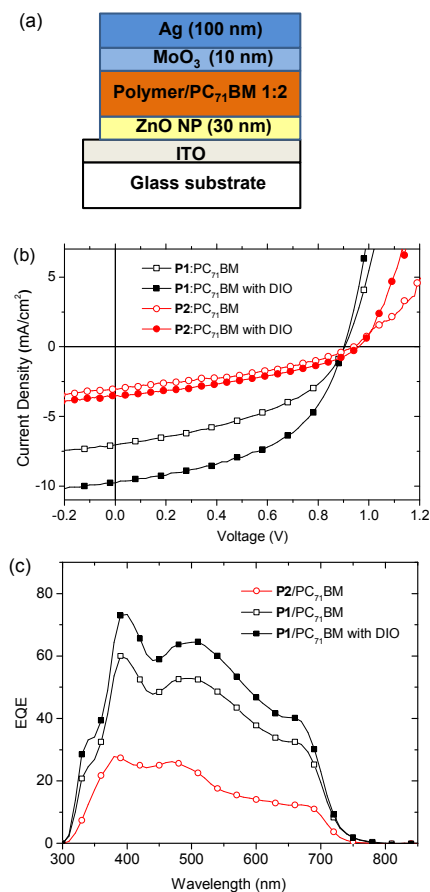


Fig. 4 (a) Schematic diagram of the BHJ solar cells. (b) *J-V* characteristics of photovoltaic devices fabricated with **P1**/PC₇₁BM (black) and **P2**:PC₇₁BM (red) under AM 1.5G irradiation (100 mW cm⁻²). (c) EQE curves of the **P1** (red) and **P2** (black) based BHJ solar cells.

The **P2**:PC₇₁BM (1:2) based solar cells showed lower performance compared to the **P1** devices with PCE of 1% (Table 2). The introduction of two fluorine atoms to the polymer unit indeed increased the *V*_{oc} and the results were consistent with the HOMO energy levels obtained by CV studies. However, the *J*_{sc} and the FF of the devices were low.^{40, 41} Solvent additive (DIO) and thermal annealing was also tested in the **P2**:PC₇₁BM device (Table 2). However, the influence of the solvent additive was not as significant as in the **P1** based solar cells.

Table 2 Photovoltaic performance of the polymer:PC₇₁BM blend films.^a

Active layer	<i>V</i> _{oc} (V)	<i>J</i> _{sc} (mA cm ⁻²)	FF	PCE (%)
P1 :PC ₇₁ BM (1:2) ^b	0.90 ± 0.01	6.8 ± 0.3	42 ± 2	2.60 ± 0.20
P1 :PC ₇₁ BM (1:2) ^{b,c}	0.90 ± 0.01	9.7 ± 0.2	47 ± 2	4.20 ± 0.20
P2 :PC ₇₁ BM (1:2) ^b	0.92 ± 0.02	3.0 ± 0.1	36 ± 1	1.00 ± 0.10
P2 :PC ₇₁ BM (1:2) ^{b,c}	0.94 ± 0.01	3.5 ± 0.1	36 ± 1	1.20 ± 0.10

^a Solar cell performance of inverted structure devices. Average values (10 devices) shown with standard deviation. ^b Weight ratio. ^c With 2.5% of DIO and thermally annealed at 120 °C for 3 min.

The external quantum efficiencies (EQEs) of the solar cell devices were also studied. Fig. 4c shows the EQE curves of the solar cells fabricated under the same optimized conditions as those used for the *J-V* measurements. Clearly, the EQE values for **P1** are higher than those of **P2** based solar cells, which agree with the higher *J*_{sc} values of the devices derived from **P1**.

Space-charge-limited current (SCLC) measurement was conducted to study the hole and electron mobility of the polymer/PC₇₁BM blend films (Fig. S7 and S8). Hole only and electron only devices were fabricated (see ESI for details). According to Mott-Gurney law, SCLC theory can be described as $J = 9\epsilon_0\epsilon_r\mu(V_a - V_{bi})^2/8d^3$, where *J* is current density, ϵ_0 is permittivity of vacuum, ϵ_r is relative permittivity of the material, μ is mobility, *V*_a is applied voltage, *V*_{bi} is built-in voltage, and *d* is the thickness of the active film.^{42, 43} By this method, the hole mobility of **P1**:PC₇₁BM (1:2) blend film was determined to be 1.3×10^{-5} cm² V⁻¹ s⁻¹ which was higher than that of the **P2**:PC₇₁BM (1:2) blend film (6.9×10^{-6} cm² V⁻¹ s⁻¹) (Fig. S7). The electron mobility of the blends films were similar in the 10⁻⁴ cm² V⁻¹ s⁻¹ range (Fig. S8). This means that the charge transport in the **P1**:PC₇₁BM film was more balanced than that of the **P2**:PC₇₁BM film. The result correlated to the higher *J*_{sc} obtained from the **P1** based solar cell devices.

The surface morphology of the polymer:PC₇₁BM blend films were investigated using tapping mode AFM and the images are shown in Fig. 5. Compared to the blend film of **P2**:PC₇₁BM which gave lower FF and *J*_{sc}, **P1**:PC₇₁BM blend film displayed a clear, phase-separated morphology in the nanometre scale. Nanometre phase separation is thought to be good for charge separation and transport as evidenced in many high performance polymers.⁴⁴⁻⁴⁶ The blend film of **P1**:PC₇₁BM with DIO as solvent additive was also studied which gave even more evident phase separation. The percolated biphasic structure showed domain sizes in several tens of nanometres. Such phase separated film morphology should contain large donor/acceptor interface for exciton dissociation, small-enough domains that ensure all the photogenerated excitons have chances to move to donor/acceptor interface, and effective transportation pathways for both hole and electron carriers.^{47, 48} The changes induced by addition of DIO could be due to the preferential interaction of DIO with the alkyl

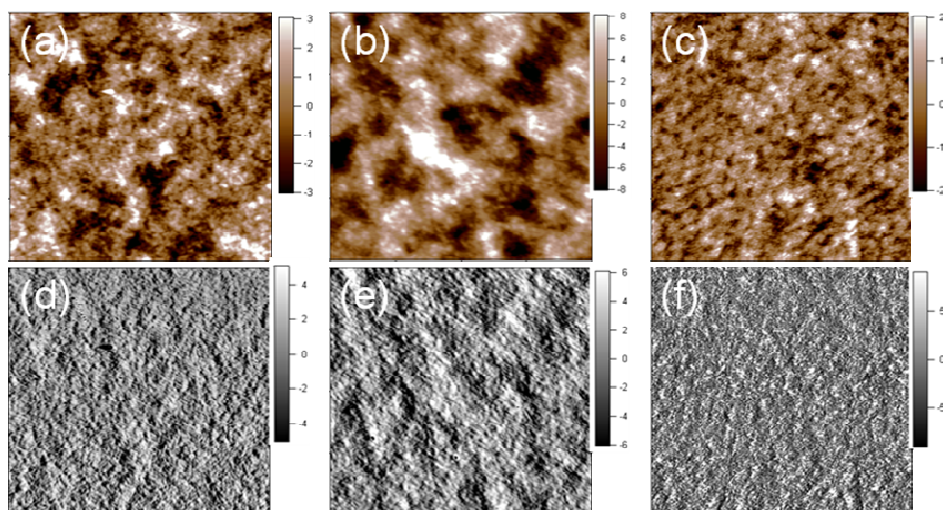


Fig. 5 AFM images of films spin coated from **P1**/PC₇₁BM 1:2 (a and d), **P1**/PC₇₁BM 1:2 with 2.5% DIO (b and e) and **P2**/PC₇₁BM 1:2 (c and f). (a), (b) and (c) are height images; (d), (e) (f) are phase images. All images are 2 × 2 μm.

substituents of the benzodithiophene repeat unit which affects the morphology of the blends.^{16, 49}

Conclusions

A new BDT unit, 4,8-bis((2-(2-ethylhexyl)-3-hexylthieno[3,2-b]thiophene) BDT, was designed, synthesized, and applied for the construction of donor-acceptor conjugated copolymers. Compared with the polymers with extended fused-ring systems along the polymer backbone,^{12-14, 50} the newly synthesized polymers featured extending fused-ring systems in a 2D manner by substituting thiophene with thieno[3,2-b]thiophene. Copolymerization of the new BDT unit with BT or fBT provided polymers with broad absorption in the visible light region and low-lying HOMO energy levels. Application of these polymers in BHJ solar cells provided high V_{oc} of 0.90 V and optimization of the solar cells by solvent additives gave PCE of 4.20%. This is close to the performance of the dithienyl-BDT analogue of similar molecular weight range.⁵³ Compared with the fused dithienobenzodithiophene system,¹² polymer **P1** showed reasonable performance indicating that using fused ring units orthogonal to the polymer backbone is a promising strategy for future polymer design.

Experimental

Unless noted, all materials were reagent grade and used as received without further purification. Compound **6** was synthesized following literature procedures.^{51, 52} All the other starting compounds and reagents are commercially available. Experimental methods and instruments can be found in the Supplementary Information.

2-(2-Ethylhexyl)-3-hexylthieno[3,2-b]thiophene (7). To a stirred mixture of Mg (0.84 g, 35 mmol) and catalytic amount of iodine in dry Et₂O (30 mL) was added ethylhexyl bromide (5.79 g, 30 mmol) dropwisely. After addition, the mixture was stirred at reflux for another 2 h. The resulting Grignard reagent was transferred dropwisely to another flask containing Pd(dppf)Cl₂

(200 mg) and compound **6** (6.06 g, 20 mmol) in dry Et₂O (30 mL) at 0 °C. After addition of the Grignard reagent, the reaction mixture was reacted at 0 °C for 2h, room temperature for 2 h and reflux 2h. After cooling to room temperature, the reaction mixture was quenched with ice slowly. The organic phase was washed with H₂O, evaporated solvent under vacuum and the residue was passed a short column (silica gel, petroleum ether) to remove the catalyst. Pure compound **7** was obtained as colorless oil after high vacuum distillation (3.3 g, 49%). Rf 0.83 (petroleum ether); IR (neat) ν 2956, 2924, 2856, 1458, 1378, 910, 707 cm⁻¹; ¹H NMR (δ, CDCl₃) 7.25 (d, $J = 5.6$ Hz, 1 H), 7.17 (d, $J = 5.6$ Hz, 1 H), 2.72 (d, $J = 6.8$ Hz, 2 H), 2.65 (t, $J = 7.6$ Hz, 2 H), 1.68 (m, 3 H), 1.25-1.40 (m, 14 H), 0.89 (m, 9 H); ¹³C NMR (δ, CDCl₃) 140.6, 140.3, 135.1, 130.4, 124.7, 119.8, 41.8, 33.2, 32.5, 31.6, 29.3, 28.9, 28.8, 28.1, 25.6, 23.0, 22.6, 14.1, 14.0, 10.9; MS (ESI⁺) m/z 336 [M]⁺; HRMS (ESI⁺) m/z calcd. for C₂₀H₃₂S₂, 336.1940 found. 336.1950.

4,8-Bis((2-(2-ethylhexyl)-3-hexylthieno[3,2-b]thiophene) BDT (8). A solution of compound **7** (1.01 g, 3.0 mmol) in THF (10 mL) was cooled to -78 °C. *n*-BuLi (2.4 M, 1.5 mL) was added slowly and the mixture was stirred for 3 h at room temperature. A suspension of 4,8-dihydrobenzene[1,2-b:4,5-b']dithiophen-4, 8-dione (220 mg, 1.0 mmol) in THF (10 mL) was then added and the mixture was stirred and slowly warmed to room temperature. A solution of SnCl₂ (758 g, 5 mmol) in 10% HCl (10 mL) was added and the mixture was stirred at 60 °C overnight. After cool to room temperature, most solvent was removed and the residue was dissolved in Et₂O, washed with 1 M HCl and H₂O. After removal of the solvent, the product was purified by column chromatography (SiO₂, petroleum ether) as a yellow solid (620 mg, 72%). Rf 0.40 (petroleum ether); mp 63-65 °C; IR (neat) ν 2957, 2924, 2854, 1457, 1377, 812, 739 cm⁻¹; ¹H NMR (CDCl₃) δ (ppm): 7.73 (d, $J = 6.0$ Hz, 2 H), 7.58 (s, 2 H), 7.49 (d, $J = 6.0$ Hz, 2 H), 2.79 (d, $J = 6.4$ Hz, 4 H), 2.72 (t, $J = 7.6$ Hz, 4 H), 1.75 (m, 4 H), 1.68 (m, 2H), 1.28-1.50 (m, 28 H), 0.90 (m, 18 H); ¹³C NMR (CDCl₃) δ (ppm): 141.1, 141.0, 139.4, 138.8, 136.8, 135.2, 130.8, 127.8, 124.3, 123.4, 120.7, 41.8, 33.3, 32.6, 31.6, 29.4, 28.9, 28.2, 25.6, 23.1, 22.6, 14.2, 14.1, 10.9; MS (ESI⁺): 858

[M]⁺. HRMS (ESI⁺) *m/z* calcd. for C₅₀H₆₆S₆: 858.3483, found 858.3491.

2,6-Bis(trimethyltin)-4,8-bis((2-(2-ethylhexyl)-3-hexylthieno[3,2-b]thiophene) BDT (9). A solution of compound **8** (430 mg, 0.5 mmol) in THF (10 mL) was cooled in a dry ice bath. *n*-BuLi (2.4 M, 0.5 mL) was added slowly and the mixture was stirred at room temperature for 2 h. SnMe₃Cl in THF (1M, 2 mL) was added and the mixture was stirred overnight. H₂O was added and the reaction mixture was extracted with hexane. After removal of solvent the product was recrystallized from CH₂Cl₂/isopropanol in fridge as a yellow solid (250 mg, 42%). Rf 0.60 (petroleum spirits); mp (toxic, decompose); IR (neat) ν 2955, 2924, 2856, 1457, 1377, 894, 826, 760, 721 cm⁻¹; ¹H NMR (CDCl₃) δ (ppm): 7.76 (s, 2 H), 7.58 (s, 2 H), 2.80 (m, 4 H), 2.74 (t, *J* = 7.6 Hz, 4 H), 1.76 (m, 4 H), 1.58 (m, 2 H), 1.30-1.50 (m, 28 H), 0.90 (m, 18 H), 0.40 (s, 18 H). ¹³C NMR (CDCl₃) δ (ppm): 143.7, 142.8, 140.9, 140.8, 139.7, 137.5, 135.2, 131.1, 130.8, 122.6, 120.5, 41.8, 33.3, 32.6, 31.7, 29.4, 28.9, 28.2, 25.6, 23.1, 22.6, 14.2, 14.1, 10.9. MS (ESI): 1186 [M]⁺. HRMS (ESI⁺) *m/z* calcd. for C₅₆H₈₂S₆Sn₂: 1186.2788, found 1186.2823 [M]⁺.

2,6-Diiodo-4,8-bis((2-(2-ethylhexyl)-3-hexylthieno[3,2-b]thiophene) BDT (10). A solution of compound **8** (430 mg, 0.5 mmol) in THF (10 mL) was cooled in dry ice-acetone bath. *n*-BuLi (2.4 M, 0.5 mL) was added slowly and the mixture was stirred at room temperature for 2 h. Iodine (300 mg, 1.2 mmol) in THF (10 mL) was added and the mixture was stirred overnight. H₂O was added and the reaction mixture was extracted with hexane. After removal of solvent, the product was purified by column chromatography (SiO₂, petroleum ether) as a yellow solid (420 mg, 76%). Rf 0.25 (petroleum spirits); mp 147-149 °C; IR (neat) ν 2955, 2924, 2853, 1456, 1365, 1175, 923, 898, 818 cm⁻¹; ¹H NMR (CDCl₃) δ (ppm): 7.85 (s, 2 H), 7.49 (s, 2 H), 2.79 (d, *J* = 6.8 Hz, 4 H), 2.74 (t, *J* = 7.6 Hz, 4 H), 1.74 (m, 4 H), 1.67 (m, 2 H), 1.30-1.50 (m, 28 H), 0.90 (m, 18 H); ¹³C NMR (CDCl₃) δ (ppm): 143.7, 141.7, 141.2, 137.6, 137.3, 135.3, 133.1, 121.7, 120.8, 80.8, 41.8, 33.3, 32.5, 31.6, 29.4, 28.9, 28.2, 25.6, 23.1, 22.6, 14.2, 14.1, 10.9. MS (ESI): 1110 [M]⁺. HRMS (ESI⁺) *m/z* calcd. for C₅₀H₆₄I₂S₆: 1110.1416, found 1110.1414 [M]⁺.

Polymer P1. The diiodo compound **10** (0.1 mmol), 4,7-bis(4,4,5,5-tetramethyl-1,3,2-dioxaborolan-2-yl)benzo[c][1,2,5]-thiadiazole (BT) (compound **11**, 0.1 mmol), 4 mol% of Pd₂(dba)₃ and 32 mol% of P(*o*-tolyl)₃ was added to a vial. A drop of the Aliquat 336 was added as phase transfer catalyst. Under nitrogen, dry toluene (1 mL) was added as solvent and 2 M Na₂CO₃ (1 mL, aqueous) was added as the base. The mixture was degassed with nitrogen for 10 min and then heated to 90 °C. After 30 min, phenylboronic acid was added and the polymer was end capped for 1 hour followed by end capping with bromobenzene for another 1 hour. Then the reaction mixture was cooled to room temperature, and the polymer was precipitated by addition of 50 mL methanol, filtered through a Soxhlet thimble. The precipitate was then subjected to Soxhlet extraction with methanol, hexanes, dichloromethane and chloroform. The residue was dissolved in *o*-dichlorobenzene (ODCB) and filtered. The filtrate was precipitated in methanol and the solid was collected and dried under vacuum. Yield: 43%. M_n = 28,900 g/mol, PDI = 1.9; IR (neat) ν 2922, 2854, 1456, 1377, 1186, 821, 721 cm⁻¹; ¹H NMR

(CDCl₃) δ (ppm): 8.50-9.50 (2 H, br), 7.50--8.50 (2 H, br), 2.50-3.50 (8 H, br), 0.80-2.00 (54 H, br).

Polymer P2. The bis(trimethyltin) compound **9** (0.1 mmol) and 5,6-difluoro-4,7-diiodobenzo[c][1,2,5]thiadiazole (fBT) (0.1 mmol) were mixed in 1 mL of toluene and 0.2 mL DMF. After being purged with nitrogen for 5 min, Pd(PPh₃)₄ (5 mg) was added as the catalyst, and the mixture was then purged with nitrogen for another 10 min. The reaction mixture was stirred and heated to 120 °C for 2 days. Phenyl trimethyltin was added and the polymer was end capped for 1 hour followed by end capping with bromobenzene for another 1 hour. Then the reaction mixture was cooled to room temperature, and the polymer was precipitated by addition of 50 mL methanol, filtered through a Soxhlet thimble. The precipitate was then subjected to Soxhlet extraction with methanol, hexanes, dichloromethane and chloroform. The polymer was recovered as solid from the chloroform fraction by precipitation from methanol. The solid polymer was dried under vacuum. Yield: 39%. M_n = 10,500 g/mol, PDI = 3.3; IR (neat) ν 2922, 2853, 1435, 1376, 1011, 800, 722 cm⁻¹; ¹H NMR (CDCl₃) δ (ppm): 7.50-8.00 (2 H, br), 2.50-3.50 (8 H, br), 0.80-2.00 (54 H, br). Elemental analysis calcd (%) for C₅₆H₆₄F₂N₂S₇: C 65.46, H 6.28, N, 2.73; found: C 65.67, H 6.17, N, 2.56.

Fabrication and characterization of the BHJ polymer solar cells. Polymer solar cells were processed on pre-patterned indium tin oxide (ITO) coated glass substrates with a sheet resistance of 15 Ω per square. First a thin layer of ZnO nanoparticle (30 nm) was deposited on the ultrasonically cleaned ITO substrates by spin coating (25 mg/mL in ethanol, 3000 rpm). ZnO nanoparticles were synthesized by a sol-gel method using zinc acetate dihydrate and tetramethylammonium hydroxide.⁵⁴ The active layer of the devices was deposited by spin coating *o*DCB solution containing 10 mg of polymer and 20 mg of PC₇₁BM. The films were then transferred to a metal evaporation chamber and MoO₃ (10 nm) and Ag (100 nm) were deposited through a shadow mask (active area was 0.1 cm²) at approximately 1 × 10⁻⁶ torr. Film thickness was determined by Veeco Dektak 150+Surface Profiler. The current density-voltage measurements of the devices were carried out using a 1 kW Oriel solar simulator with an AM 1.5G filter as the light source in conjunction with a Keithley 2400 source measurement unit. Solar measurements were carried out under 1000 W/m² AM 1.5G illumination conditions. For accurate measurement, the light intensity was calibrated using a reference silicon solar cell (PV measurements Inc.) certified by the National Renewable Energy Laboratory.

Acknowledgements

This work was made possible by support of the Victorian Organic Solar Cell Consortium, with funding provided by the Victorian State Government Department of Primary Industries (Energy Technology Innovation Strategy), Australian Renewable Energy Agency (ARENA Project 2-A018) and the Victorian State Government Department of Business Innovation (Victorian Science Agenda). Dr W. W. H. Wong is supported by an Australian Research Council Future Fellowship (FT130100500). The authors thank Dr Tianshi Qin (CSIRO) for acquiring the HT-GPC data.

Notes and references

^a School of Chemistry, Bio21 Institute, the University of Melbourne, 30 Flemington Road, Parkville, Victoria 3010, Australia. Fax: +61 3 83442384; Tel: +61 3 90356154;

[†] Electronic Supplementary Information (ESI) available. See DOI: 10.1039/b000000x/.

1. Y. Li, *Acc. Chem. Res.*, 2012, 45, 723-733.
2. S. Günes, H. Neugebauer and N. S. Sariciftci, *Chem. Rev.*, 2007, 107, 1324-1338.
3. Y.-J. Cheng, S.-H. Yang and C.-S. Hsu, *Chem. Rev.*, 2009, 109, 5868-5923.
4. Z. He, C. Zhong, S. Su, M. Xu, H. Wu and Y. Cao, *Nat. Photon.*, 2012, 6, 591-595.
5. G. Li, R. Zhu and Y. Yang, *Nat. Photon.*, 2012, 6, 153-161.
6. Z. B. Henson, K. Mullen and G. C. Bazan, *Nat. Chem.*, 2012, 4, 699-704.
7. R. A. J. Janssen and J. Nelson, *Adv. Mater.*, 2013, 25, 1847-1858.
8. Y. Li and Y. Zou, *Adv. Mater.*, 2008, 20, 2952-2958.
9. J. Hou, Z. a. Tan, Y. Yan, Y. He, C. Yang and Y. Li, *J. Am. Chem. Soc.*, 2006, 128, 4911-4916.
10. J. Hou, C. Yang, C. He and Y. Li, *Chem. Commun.*, 2006, 871-873.
11. L. Huo, S. Zhang, X. Guo, F. Xu, Y. Li and J. Hou, *Angew. Chem. Int. Ed.*, 2011, 50, 9697-9702.
12. H. J. Son, L. Lu, W. Chen, T. Xu, T. Zheng, B. Carsten, J. Strzalka, S. B. Darling, L. X. Chen and L. Yu, *Adv. Mater.*, 2013, 25, 838-843.
13. Y.-X. Xu, C.-C. Chueh, H.-L. Yip, F.-Z. Ding, Y.-X. Li, C.-Z. Li, X. Li, W.-C. Chen and A. K. Y. Jen, *Adv. Mater.*, 2012, 24, 6356-6361.
14. H. Zhong, Z. Li, F. Deledalle, E. C. Fregoso, M. Shahid, Z. Fei, C. B. Nielsen, N. Yaacobi-Gross, S. Rossbauer, T. D. Anthopoulos, J. R. Durrant and M. Heeney, *J. Am. Chem. Soc.*, 2013, 135, 2040-2043.
15. L. Huo and J. Hou, *Polym. Chem.*, 2011, 2, 2453-2461.
16. R. S. Kularatne, P. Sista, H. Q. Nguyen, M. P. Bhatt, M. C. Biewer and M. C. Stefan, *Macromolecules*, 2012, 45, 7855-7862.
17. Z. Xiao, J. Subbiah, K. Sun, S. Ji, D. J. Jones, A. B. Holmes and W. H. Wong, *J. Mater. Chem. C*, 2014, 2, 1306-1313.
18. W. W. H. Wong, J. Subbiah, S. R. Puniredd, W. Pisula, D. J. Jones and A. B. Holmes, *Polym. Chem.*, 2014, 5, 1258-1263.
19. M. Wang, X. Hu, P. Liu, W. Li, X. Gong, F. Huang and Y. Cao, *J. Am. Chem. Soc.*, 2011, 133, 9638-9641.
20. I. McCulloch, M. Heeney, M. L. Chabiny, D. DeLongchamp, R. J. Kline, M. Cölle, W. Duffy, D. Fischer, D. Gundlach, B. Hamadani, R. Hamilton, L. Richter, A. Salleo, M. Shkunov, D. Sparrowe, S. Tierney and W. Zhang, *Adv. Mater.*, 2009, 21, 1091-1109.
21. B. S. Rolczynski, J. M. Szarko, H. J. Son, Y. Liang, L. Yu and L. X. Chen, *J. Am. Chem. Soc.*, 2012, 134, 4142-4152.
22. C. Risko, M. D. McGehee and J.-L. Bredas, *Chem. Sci.*, 2011, 2, 1200-1218.
23. S. S. Zade and M. Bendikov, *Angew. Chem. Int. Ed.*, 2010, 49, 4012-4015.
24. N. Wang, Z. Chen, W. Wei and Z. Jiang, *J. Am. Chem. Soc.*, 2013, 135, 17060-17068.
25. H. Zhou, L. Yang, A. C. Stuart, S. C. Price, S. Liu and W. You, *Angew. Chem. Int. Ed.*, 2011, 50, 2995-2998.
26. L. Yang, H. Zhou, S. C. Price and W. You, *J. Am. Chem. Soc.*, 2012, 134, 5432-5435.
27. Z. Li, J. Lu, S.-C. Tse, J. Zhou, X. Du, Y. Tao and J. Ding, *J. Mater. Chem.*, 2011, 21, 3226-3233.
28. Z. Fei, J. S. Kim, J. Smith, E. B. Domingo, T. D. Anthopoulos, N. Stingelin, S. E. Watkins, J.-S. Kim and M. Heeney, *J. Mater. Chem.*, 2011, 21, 16257-16263.
29. B. Carsten, F. He, H. J. Son, T. Xu and L. Yu, *Chem. Rev.*, 2011, 111, 1493-1528.
30. T. Umeyama, Y. Watanabe, E. Douvogianni and H. Imahori, *J. Phys. Chem. C*, 2013, 117, 21148-21157.
31. Y. Wang, X. Xin, Y. Lu, T. Xiao, X. Xu, N. Zhao, X. Hu, B. S. Ong and S. C. Ng, *Macromolecules*, 2013, 46, 9587-9592.
32. Y. Zou, A. Najari, P. Berrouard, S. Beaupré, B. Réda Aïch, Y. Tao and M. Leclerc, *J. Am. Chem. Soc.*, 2010, 132, 5330-5331.
33. P. J. Brown, D. S. Thomas, A. Köhler, J. S. Wilson, J.-S. Kim, C. M. Ramsdale, H. Sirringhaus and R. H. Friend, *Phys. Rev. B: Condens. Matter*, 2003, 67, 064203.
34. C. M. Cardona, W. Li, A. E. Kaifer, D. Stockdale and G. C. Bazan, *Adv. Mater.*, 2011, 23, 2367-2371.
35. J. Yuan, Z. Zhai, H. Dong, J. Li, Z. Jiang, Y. Li and W. Ma, *Adv. Funct. Mater.*, 2013, 23, 885-892.
36. G. Dennler, M. C. Scharber and C. J. Brabec, *Adv. Mater.*, 2009, 21, 1323-1338.
37. Y. Zhang, Z. Li, S. Wakim, S. Alem, S.-W. Tsang, J. Lu, J. Ding and Y. Tao, *Org. Electron.*, 2011, 12, 1211-1215.
38. J. K. Lee, W. L. Ma, C. J. Brabec, J. Yuen, J. S. Moon, J. Y. Kim, K. Lee, G. C. Bazan and A. J. Heeger, *J. Am. Chem. Soc.*, 2008, 130, 3619-3623.
39. Y. Huang, X. Guo, F. Liu, L. Huo, Y. Chen, T. P. Russell, C. C. Han, Y. Li and J. Hou, *Adv. Mater.*, 2012, 24, 3383-3389.
40. T.-Y. Chu, J. Lu, S. Beaupré, Y. Zhang, J.-R. Pouliot, J. Zhou, A. Najari, M. Leclerc and Y. Tao, *Adv. Funct. Mater.*, 2012, 22, 2345-2351.
41. L. Dou, C.-C. Chen, K. Yoshimura, K. Ohya, W.-H. Chang, J. Gao, Y. Liu, E. Richard and Y. Yang, *Macromolecules*, 2013, 46, 3384-3390.
42. Y. Fu, H. Cha, G.-Y. Lee, B. J. Moon, C. E. Park and T. Park, *Macromolecules*, 2012, 45, 3004-3009.
43. C.-M. Yang, H.-H. Liao, S.-F. Horng, H.-F. Meng, S.-R. Tseng and C.-S. Hsu, *Synth. Met.*, 2008, 158, 25-28.
44. Y. Liang, Z. Xu, J. Xia, S.-T. Tsai, Y. Wu, G. Li, C. Ray and L. Yu, *Adv. Mater.*, 2010, 22, E135-E138.
45. J. Peet, J. Y. Kim, N. E. Coates, W. L. Ma, D. Moses, A. J. Heeger and G. C. Bazan, *Nat. Mater.*, 2007, 6, 497-500.
46. S. Kouijzer, J. J. Michels, M. van den Berg, V. S. Gevaerts, M. Turbiez, M. M. Wienk and R. A. J. Janssen, *J. Am. Chem. Soc.*, 2013, 135, 12057-12067.
47. L. Dong, W. Li and W.-S. Li, *Nanoscale*, 2011, 3, 3447-3461.
48. C.-Y. Mei, L. Liang, F.-G. Zhao, J.-T. Wang, L.-F. Yu, Y.-X. Li and W.-S. Li, *Macromolecules*, 2013, 46, 7920-7931.
49. S. Albrecht, S. Janietz, W. Schindler, J. Frisch, J. Kurpiers, J. Kniepert, S. Inal, P. Pingel, K. Fostiropoulos, N. Koch and D. Neher, *J. Am. Chem. Soc.*, 2012, 134, 14932-14944.
50. H.-J. Yun, Y.-J. Lee, S.-J. Yoo, D. S. Chung, Y.-H. Kim and S.-K. Kwon, *Chem. Eur. J.*, 2013, 19, 13242-13248.
51. M. He and F. Zhang, *J. Org. Chem.*, 2006, 72, 442-451.

-
52. W. Tang, S. P. Singh, K. H. Ong and Z.-K. Chen, *J. Mater. Chem.*, 2010, 20, 1497-1505.
53. The study on the dithienyl-BDT anaolgue of **PI** will be published elsewhere.
54. G. Sarasqueta, K. R. Choudhury, J. Subbiah, F. So, *Adv. Funct. Mater.*, 2011, 21, 167-171.